GPS and seismological constraints on active tectonics and arc-continent collision in Papua New Guinea: Implications for mechanics of microplate rotations in a plate boundary zone

Laura M. Wallace,[1,2] Colleen Stevens,[3,4] Eli Silver,[1] Rob McCaffrey,[3] Wesley Loratung,[5] Suvenia Hasiata,[6] Richard Stanaway,[7] Robert Curley,[6] Robert Rosa,[5] and Jones Taugaloidi[6]

Received 3 March 2003; revised 23 October 2003; accepted 28 January 2004; published 18 May 2004.

[1] The island of New Guinea is located within the deforming zone between the Pacific and Australian plates that converge obliquely at ~110 mm/yr. New Guinea has been fragmented into a complex array of microplates, some of which rotate rapidly about nearby vertical axes. We present velocities from a network of 38 Global Positioning System (GPS) sites spanning much of the nation of Papua New Guinea (PNG). The GPS-derived velocities are used to explain the kinematics of major tectonic blocks in the region and the nature of strain accumulation on major faults in PNG. We simultaneously invert GPS velocities, earthquake slip vectors on faults, and transform orientations in the Woodlark Basin for the poles of rotation of the tectonic blocks and the degree of elastic strain accumulation on faults in the region. The data are best explained by six distinct tectonic blocks: the Australian, Pacific, South Bismarck, North Bismarck, and Woodlark plates and a previously unrecognized New Guinea Highlands Block. Significant portions of the Ramu-Markham Fault appear to be locked, which has implications for seismic hazard determination in the Markham Valley region. We also propose that rapid clockwise rotation of the South Bismarck plate is controlled by edge forces initiated by the collision between the Finisterre arc and the New Guinea Highlands. *INDEX TERMS:* 8150 Tectonophysics: Plate boundary—general (3040); 8110 Tectonophysics: Continental tectonics—general (0905); 1243 Geodesy and Gravity: Space geodetic surveys; 1206 Geodesy and Gravity: Crustal movements—interplate (8155); *KEYWORDS:* Papua New Guinea, GPS, microplate, tectonics, collision

Citation: Wallace, L. M., C. Stevens, E. Silver, R. McCaffrey, W. Loratung, S. Hasiata, R. Stanaway, R. Curley, R. Rosa, and J. Taugaloidi (2004), GPS and seismological constraints on active tectonics and arc-continent collision in Papua New Guinea: Implications for mechanics of microplate rotations in a plate boundary zone, *J. Geophys. Res.*, *109*, B05404, doi:10.1029/2003JB002481.

1. Introduction

[2] Complex tectonic plate interactions can arise between multiple, rapidly rotating microplates in the deforming zone between major, fast moving plates. The boundaries between these rotating microplates are often the sites of major collisional orogenies, subduction zones, rift systems, and rapidly slipping transform faults. Use of Global Positioning System (GPS) techniques in recent years has allowed more accurate quantification of microplate rotations and interactions in plate boundary zones [e.g., *Tregoning et al.*, 1998; *Stevens et al.*, 1999, 2002; *McClusky et al.*, 2000; *McCaffrey et al.*, 2000]. GPS data can also be used to evaluate the nature of strain accumulation along faults in these plate boundary zones. Moreover, if we are able to assess the effects of elastic strain and tectonic block rotations on GPS site velocities concurrently, then we can better quantify the kinematics of tectonic blocks caught up in plate boundary zones. Understanding the kinematics of these microplates can potentially help us resolve long-standing questions about the forces driving microplate rotation.

[3] Because it is composed of microplates that rotate rapidly about nearby axes, the island nation of Papua New Guinea (PNG) contains every type of plate boundary imaginable (Figure 1). The relative motions across these block boundaries in PNG are fast, making GPS an ideal tool for obtaining information about the active tectonic regime. We present the results of seven GPS campaigns undertaken

[1]Earth Sciences Department, University of California, Santa Cruz, California, USA.
[2]Now at Institute of Geological and Nuclear Sciences, Lower Hutt, New Zealand.
[3]Department of Earth and Environmental Sciences, Rensselaer Polytechnic Institute, Troy, New York, USA.
[4]Now at Geographic Data Technology, Lebanon, New Hampshire, USA.
[5]Papua New Guinea National Mapping Bureau, Port Moresby, Papua New Guinea.
[6]Papua New Guinea University of Technology, Lae, Papua New Guinea.
[7]Research School of Earth Sciences, Australian National University, Canberra ACT, Australia.

0148-0227/04/2003JB002481$09.00

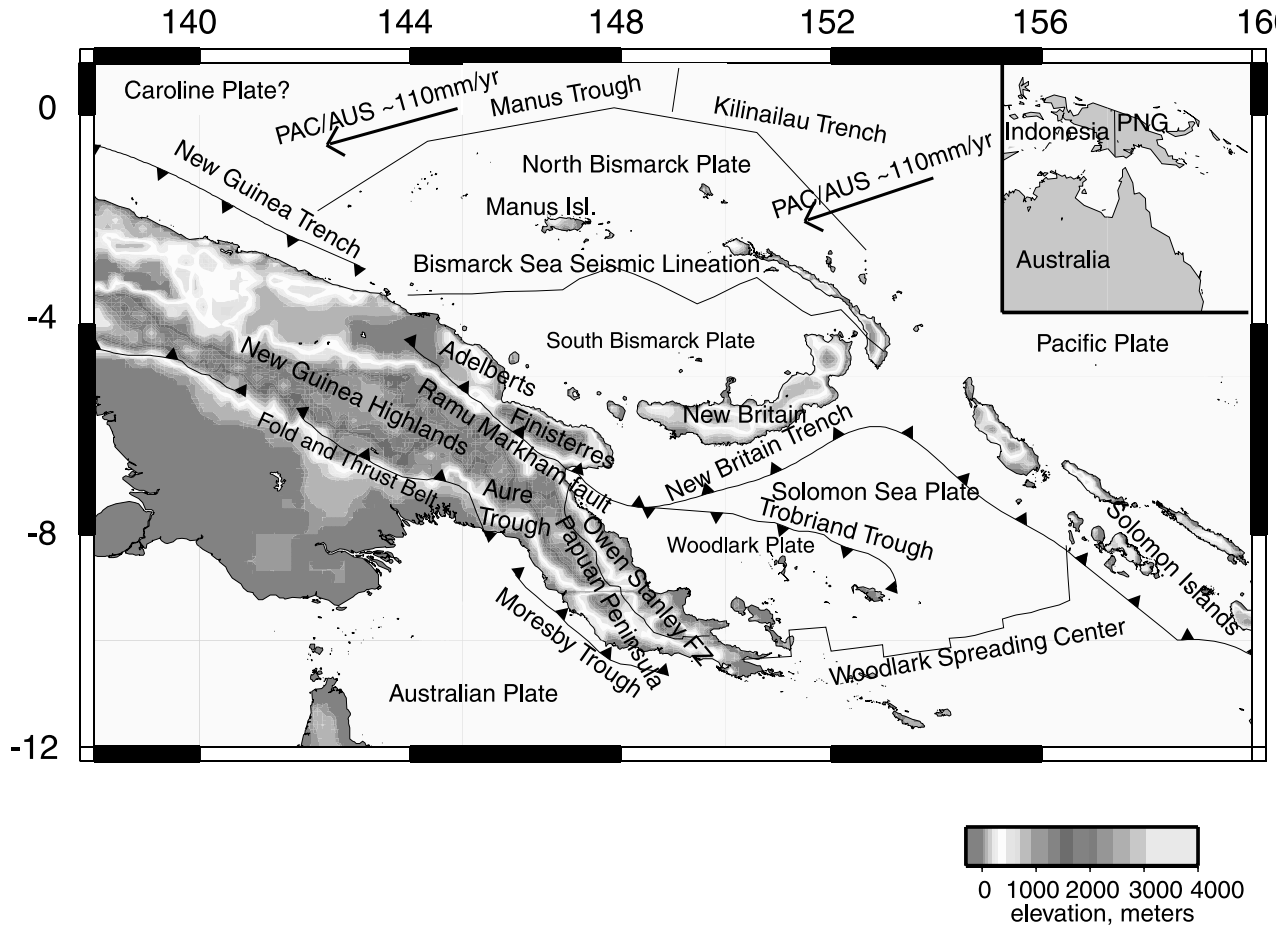

Figure 1. Tectonic setting of Papua New Guinea. Faults are mostly from *Hamilton* [1979]; the Pacific/Australia relative motion vector is from *DeMets et al.* [1990, 1994]. In the inset, PNG, Papua New Guinea. See color version of this figure in the HTML.

from 1993 to 2002 at 38 sites, largely in the northeastern part of the island of New Guinea and focused on the region surrounding the Finisterre Collision (Figure 2). We integrate these GPS data with previous GPS measurements [*Tregoning et al.*, 1998, 1999; *Tregoning*, 2002] and with geological and geophysical data from the region to gain a more complete picture of the active tectonic framework of PNG. Our resulting tectonic model of the region requires as many as six tectonic plates and microplates (Figures 1 and 3). We predict the nature of deformation across the boundaries between these tectonic blocks based on their poles of rotation and compare this to geological and geophysical evidence for active faulting. The kinematics of some of these tectonic blocks indicate that forces associated with subduction and collision are involved in the microplate rotations in the PNG region.

2. Tectonic Overview

[4] The active tectonic regime in PNG is dominated by the convergent motion of the Pacific plate which moves west-southwest at ~110 mm/yr relative to the Australian plate, oblique to the orientation of the island (Figure 1). Interactions between the Australian and Pacific plates have made PNG the site of orogenic events since at least the late Oligocene [*Dow*, 1977; *Pigram and Davies*, 1987]. Previous tectonic studies in the region have proposed that PNG is composed of several tectonic blocks: these include Australia, Pacific, South Bismarck, Solomon Sea, North Bismarck, and Woodlark plates [e.g., *Johnson and Molnar*, 1972; *Curtis*, 1973; *Taylor*, 1979; *Johnson*, 1979; *Hamilton*, 1979; *Davies et al.*, 1984].

[5] A broad array of tectonic environments is represented in PNG. A well-developed fold and thrust belt has grown over the Australian margin in the southern part of the New Guinea orogen over the last 5 Myr [*Jenkins*, 1974; *Hill and Gleadow*, 1989; *Hill and Raza*, 1999] (Figure 1). Folds at the front of the fold and thrust belt appear to be actively growing today [*Hamilton*, 1979; H. Davies, personal communication, 2001], and faults there are seismically active [*Ripper and McCue*, 1983; *Abers and McCaffrey*, 1988; *Abers*, 1989]. The Finisterre terrane in northeastern PNG is currently being emplaced onto the northern margin of the island of New Guinea, presenting a fine example of active arc-continent collision [*Jaques and Robinson*, 1977; *Johnson*, 1979; *Davies et al.*, 1987; *Silver et al.*, 1991; *Kulig et al.*, 1993; *Abers and McCaffrey*, 1994; *Abbott et al.*, 1994b]. A volcanic arc has formed off the north coast in response to active subduction along the New Britain Trench. The Woodlark spreading center represents the primary boundary between the Woodlark and Australian plates. The Woodlark Basin is opening as the Woodlark plate rotates in a counter-

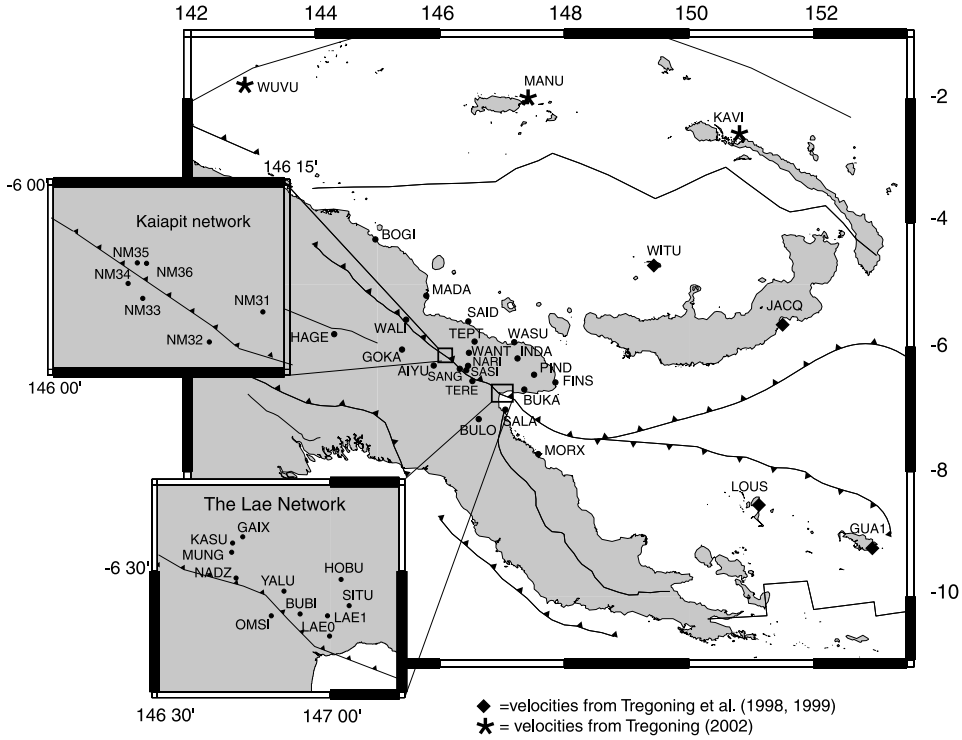

Figure 2. Map of GPS sites discussed in this paper. Insets show expanded views of the Lae and Kaiapit networks in the Markham Valley.

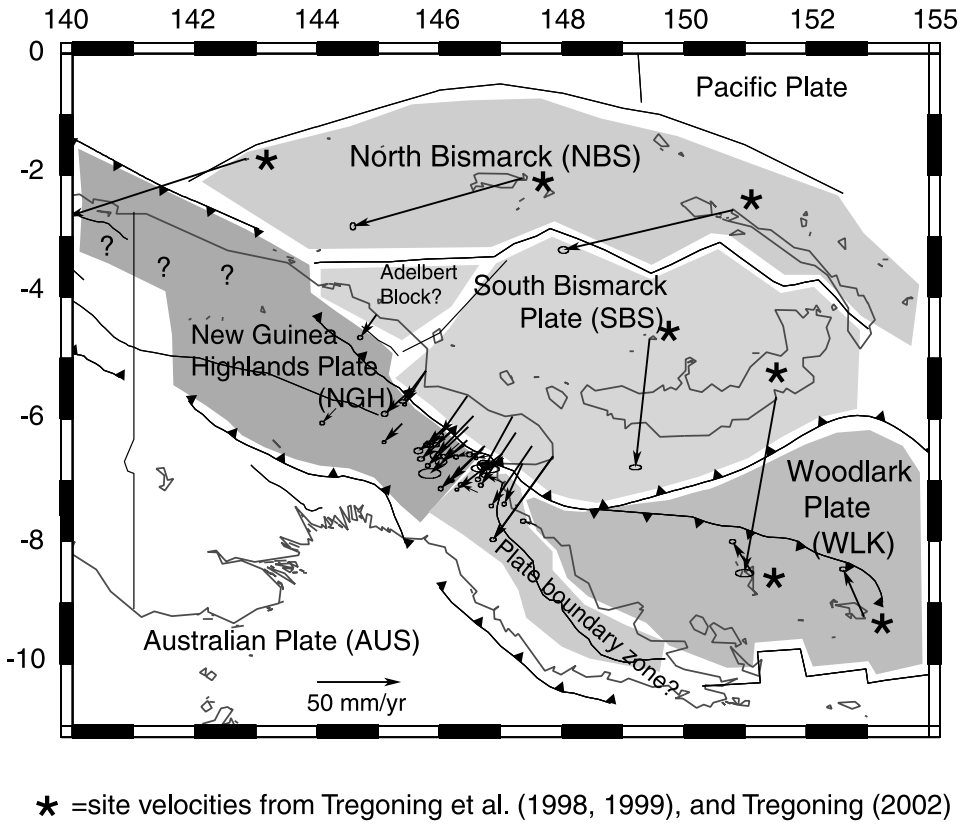

Figure 3. Tectonic block configuration in PNG and the GPS velocities relative to the Australian Plate. Note we include a possible "Adelbert Block" in this schematic model, based on a northeast trending zone of shallow strike-slip earthquakes north of Madang (see Figure 4). The GPS results are inconclusive concerning the existence of a separate Adelbert Block; in this paper we assume that the Adelbert Block is part of the South Bismarck Plate. See color version of this figure in the HTML.

clockwise manner away from the Australian plate [*Weissel et al.*, 1982; *Benes et al.*, 1994]. The Bismarck Sea Seismic Lineation to the north of New Britain is a series of left-lateral transform faults and rifts that connect the transform segments [*Denham*, 1969; *Taylor*, 1979]. The rifts have facilitated opening of the Manus Basin, and the New Guinea Basin over the last 3.5 Myr [*Taylor*, 1979] (Figure 1).

3. Previous GPS Studies in PNG

[6] GPS studies have been conducted in PNG by institutions in Australia, the United States, and PNG for the last decade [*McClusky et al.*, 1994; *Mobbs*, 1997; *Stevens et al.*, 1998; *Tregoning et al.*, 1998, 1999, 2000; *Tregoning*, 2002]. *Tregoning et al.* [1998] presented results from a network of 20 sites, including sites in New Britain, New Ireland, Manus, two sites in the Woodlark basin, and three sites on the mainland of New Guinea. They interpreted their data using two major plates (Australia, Pacific), and two minor plates (South Bismarck, Woodlark) (Figure 1). The New Guinea Highlands were assumed to be part of the stable Australian plate. This assumption was not testable at the time, as there were no site velocity estimates from the New Guinea Highlands. Their results were consistent with spreading in the Woodlark Basin, convergence along the Ramu-Markham Fault and New Britain Trench, rapid left-lateral motion and seafloor spreading along the Bismarck Sea Seismic Lineation, and left-lateral strike-slip faulting on the Papuan Peninsula. Their Woodlark/Australia pole from GPS in the Woodlark basin suggests that active spreading in the Woodlark basin is significantly slower than indicated by magnetic anomalies [*Goodliffe et al.*, 1997; *Tregoning et al.*, 1998; *Taylor et al.*, 1999]. *Stevens et al.* [1998] utilized data gathered across the Ramu-Markham Fault to measure coseismic displacements from the 1993 Kaiapit earthquakes (M_w = 6.4–6.8), and used these data in conjunction with earthquake waveform modeling to conclude that the Ramu-Markham Fault has a distinct ramp-detachment geometry.

4. GPS Data Acquisition and Processing

[7] The University of California Santa Cruz (UCSC), Rensselaer Polytechnic Institute (RPI), PNG National Mapping Bureau (NMB), and the PNG University of Technology collaborated to conduct GPS surveys in the region of the Ramu-Markham Fault in 1993, 1994, and 1997. We expanded the network in 1998 to include ~40 sites in order to focus on broader deformation throughout the northern part of the island, particularly the deformation associated with the Finisterre arc-continent collision (Figure 2). The sites installed in 1998 were observed again in 2000, and most of these were also observed in 1999, 2001, or 2002. Most of our sites have had three or more occupations with at least a year between each observation (see Table 1). Sites in the regional GPS network were observed continuously for ~4 days during each occupation period. Sites in our two local networks (the Lae and Kaiapit areas) were usually observed for a minimum of 24 hours each occupation, and most of them were occupied on at least four separate occasions (Figure 2). We used a combination of Trimble 4000SSi, Ashtech Z-XII, and Sokkia GPS instruments in the data acquisition. For most observations post-1997, we used choke ring antennas. Before 1997, dominantly Ashtech L1/L2 antennas were used. We have attempted to minimize antenna mixing in our data collection, but with campaigns spanning nearly a decade, it inevitably happens. Some of the monuments used are preexisting permanent survey marks installed by NMB, and we installed the remaining monuments as needed.

[8] We processed the GPS data using GAMIT/GLOBK software [*King and Bock*, 2002; *Herring*, 2001]. The procedure used in this type of analysis has been reviewed extensively by *Feigl et al.* [1993], *Herring et al.* [1990], *Tregoning et al.* [1998], and *McClusky et al.* [2000]. For the first stage of the processing, we estimate station coordinates, the zenith delay of the atmosphere at each station, and orbital and Earth orientation parameters (EOPs) using doubly differenced GPS phase observations. All of these parameters are loosely constrained in this step. At this stage in the processing, we also include GPS data from a few International GPS Service (IGS) sites in the region in addition to our campaign sites in PNG in order to link our network with the IGS network of sites.

[9] In order to calculate site positions and velocities in a consistent reference frame (ITRF2000) [*Altamimi et al.*, 2002], we use our loosely constrained solution (EOPs, orbital parameters, and coordinates and their covariances) from GAMIT, and we also use loosely constrained solutions (performed by Scripps Orbit and Permanent Array Center) of the global IGS network. These loosely constrained solutions are combined in GLOBK (a Kalman filter); we place tight constraints on the ITRF2000 velocities of most of the core IGS sites (Table 2) in order to align the sites in our network with ITRF2000. The fit to the core IGS sites used in the reference frame determination is shown in Table 2. Table 3 shows our PNG site velocities in an ITRF2000 reference frame, while we present our ITRF2000 velocity estimates for Australian and Pacific plate sites in Table 4. The GPS site velocities are plotted in an Australia-fixed reference frame in Figure 3. To calculate the velocities relative to Australia for Figure 3, we solve for a rotation of the data set that minimizes the velocities at the Australian plate sites.

[10] To further demonstrate that our final velocity solution is aligned with ITRF2000, Table 5 shows the difference between our velocities at IGS Australian and Pacific plate sites and the official ITRF2000 velocities of those sites, as well as a comparison between our velocities and the ITRF2000 velocities obtained by *Beavan et al.* [2002] for the same sites. *Beavan et al.* [2002] carefully aligned their network with ITRF2000 and processed much of the available data for each of those sites; our velocity estimates agree well with their results. However, our estimates for Australian and Pacific plate site velocities are not meant to be an improvement upon the results of *Beavan et al.* [2002], as they processed a larger subset of the time series of available data. Velocities for two sites in PNG that we have in common with *Tregoning et al.* [1999] agree to within 3.5 mm/yr. Daily and yearly repeatabilities of solutions for each site were very good, generally with much less than 10–20 mm of scatter. Errors in GPS site velocities are often underestimated [*Mao et al.*, 1999], due to factors like monument instability, instrument setup errors, reference frame problems, mismodeled satellite orbits, and effects from multipath. We multiply all our formal errors (output by GLOBK) by a factor of 2, for a more conservative estimate of the true uncertainties in our site velocities.

Table 1. Observation Periods for GPS Sites Used in This Paper[a]

Sites	1993	1994	1997	1998	1999	2000	2001	2002
AIYU				188	138–140	175–177		
BOGI				182–184		192–195	197–200	
BUBI	214–217, 222		100, 102	190	118, 219	201–202		
BUKA				174–177		185–188	204–206	
BULO				182–185		185–188	158–161	
FINS			99–101	195–197		185–188		
GAIX				190	219	202	204–205	
GOKA		10–12	105	181–185	123–126	193–196		
HAGE				181–184		193–195	197–200	
HOBU	218, 222		100–102	174–177	111–112, 219	185–188, 201–202	236–237	
INDA				174–177	111–112	185–188	197–198	
KASU			98	190			199	
LAE0	217, 222		100, 102				206–208	
LAE1[b]			98–105	174–197	111–148, 219–220	175–202	152–161, 197–208, 234–235	95–106, 130–132, 215–217
MADA		10–12	99–105	181–184		193–196		
MORX				174–177		185–189		
MUNG			98			202	200	
NADZ	215–216		98, 100	190	118–119, 219	201–202	158–161	
NARI						199	204–205	104–106
NM31	219	6–8	105	188		199		
NM32	219	7–8	105	188		199		
NM33	219	6–7	105	188		199		
NM34	219	6–12	105	182–185, 188		192–195, 199		
NM35	219	8–9	105	188		199		
NM36	219	6, 8	105	188		199		
OMSI	216		100, 102				206–207	
PIND				174–177				095–098
SAID				183–184		194–196		
SALA						201–202	197–198	130–132
SANG				188		199	204–205	
SASI						199	204–205	104–106
SITU	218		100, 102		117, 219	201–202	236–237	
TEPT				190–195	145–149			
TERE	216		98	190				
WALI				183–185	131–133	193–196		
WANT				182–185		185–187	197–200	
WASU				174–177		185–188	199–200	
YALU	217, 222		100, 102	190		201–202		

[a]Period in day of year.
[b]Continuously running site.

[11] Several of our GPS sites have experienced coseismic displacements. Sites NM31, NM32, NM33, NM34, NM35, and NM36 were all displaced by the 1993 Kaiapit earthquakes [*Stevens et al.*, 1998]. To determine the interseismic velocity at those sites, we only use data from 1997, 1998, and 2000. There is no noticable postseismic effect during that period, although there was some postseismic displacement at those sites during the period from 1994 to sometime before 1997. HOBU and INDA also underwent coseismic displacement due to an earthquake in mid-1999; an offset due to this displacement was estimated for these two sites, and this offset has been accounted for in our interseismic GPS velocity estimate. The GPS velocities at HOBU before and after the earthquake agree to within 6 mm/yr. There are insufficient data from INDA prior to the earthquake to estimate a preearthquake velocity.

5. Modeling the Site Velocities

[12] In order to understand the kinematics of tectonic blocks within PNG and to estimate the nature of strain accumulation along the Ramu-Markham Fault, we employ a modeling approach that simultaneously inverts for the poles of rotation for elastic, spherical blocks and locking on block-bounding faults that give the best possible fit to GPS velocities, earthquake slip vectors, transform orientations, and fault slip rate estimates. We utilize a method described by *McCaffrey* [2002] and *McCaffrey et al.* [2000] that applies simulated annealing to downhill simplex minimization [*Press et al.*, 1989] to solve for the poles and fault locking parameters. Data misfit, determined using the reduced chi-square statistic (χ^2_n), is minimized. Surface deformation due to slip on faults in the area is calculated using an elastic, half-space dislocation model [*Okada*, 1985]. It is necessary to use this approach in PNG because no point in the region is far from a plate boundary, so velocities for any of our GPS sites will reflect elastic strain as well as rigid block rotation. Here we solve for locking on the Ramu-Markham Fault, the Owen Stanley Fault Zone, the Bismarck Sea Seismic Lineation, and the Highlands Fold and Thrust Belt.

[13] We use a 10-degree uncertainty for the earthquake slip vectors directions. We chose this uncertainty because the standard error per unit weight (SEUW) for the slip vectors (in the kinematic modeling) is closest to 1 when using a 10-degree uncertainty. We obtain most of the

Table 2. IGS Sites Used for Reference Frame Stabilization in GLOBK[a]

Site	East	North
ALGO	0.14	−0.07
BRAZ	−0.87	1.35
BRMU	−0.90	0.55
DRAO	0.86	−0.12
FAIR	0.26	0.44
FORT	0.04	0.40
GODE	−0.24	0.55
GUAM	0.99	−1.25
HART	−1.97	−1.14
IRKT	−0.29	−0.02
KERG	1.02	1.04
KIT3	0.44	−0.38
KOSG	1.05	0.28
KOUR	0.67	0.41
KWJ1	1.07	0.57
LHAS	−0.83	−0.76
MADR	−0.10	−2.11
MAS1	−0.04	0.09
MATE	1.02	−0.21
MDO1	1.50	0.45
NLIB	1.53	0.07
NYAL	−1.56	−1.64
OHIG	0.15	0.77
ONSA	0.65	−0.57
PERT	−0.20	−0.41
PIE1	1.08	1.19
SANT	−1.45	1.12
SHAO	0.12	−0.86
THU1	−0.14	−0.61
TIDB	0.54	1.31
TSKB	0.76	−0.99
VILL	−0.28	−0.23
WES2	−0.47	−0.64
YAR1	−1.04	1.02
YELL	0.09	−0.01
ZWEN	0.22	−0.57

[a]East and north columns show the difference between the official ITRF00 velocity estimates at those sites and our ITRF00 velocity estimates for those sites, in mm/yr.

earthquake focal mechanism solutions from the Harvard centroid moment tensor (CMT) catalogue [*Dziewonski and Woodhouse*, 1983]. We decide which plane to use for the slip vector calculations on the basis of knowledge of active fault strikes and dips in the region from geological and geophysical studies. For example, for the Ramu-Markham Fault we only use slip vectors from events consistent with north to northeast dipping thrust earthquakes. We use slip vectors from events shallower than 40 km, as these likely represent interplate deformation. We also include relevant earthquake slip vectors from events discussed by *Abers* [1989] and *Abers and McCaffrey* [1988, 1994]. We incorporated 333 earthquake slip vectors from the New Britain Trench, Ramu-Markham Fault, the New Guinea Fold and Thrust Belt, and the Bismarck Sea Seismic Lineation (Figures 4 and 5). We include four Woodlark Basin transform orientations in the inversion, assuming an uncertainty of 1 degree for transform orientations (A. Goodliffe, personal communication, 2003). Woodlark Basin spreading has undergone a reorientation in recent times [*Goodliffe et al.*, 1997], and we use only transform orientations from the reoriented spreading center.

[14] In addition to solving for poles of rotation for tectonic blocks this method also allows us to optimally rotate GPS velocity solutions into a common reference

Table 3. Site Locations, Velocities (ITRF2000), Uncertainties, and Correlations (ρ) Between East and North Components of Velocity

			Velocity, mm/yr		2σ Uncertainty, mm/yr		
Site	Longitude	Latitude	East	North	East	North	ρ
AIYU	145.905	−6.340	26.2	49.4	2.9	1.9	0.052
BOGI	144.968	−4.295	26.5	42.8	1.9	1.6	−0.005
BUBI	146.913	−6.668	25.5	53.9	1.2	1.0	0.013
BUKA	147.356	−6.729	24.1	31.5	1.5	1.3	0.011
BULO	146.626	−7.207	24.9	60.4	1.8	1.4	−0.001
FINS	147.855	−6.615	−0.4	6.0	2.1	1.4	0.029
GAIX	146.747	−6.443	8.7	30.5	1.6	1.4	−0.005
GOKA	145.392	−6.081	24.6	45.2	1.2	1.0	0.038
HAGE	144.307	−5.832	27.4	47.9	1.6	1.3	0.003
HOBU	147.032	−6.568	8.4	33.3	1.3	1.1	−0.003
INDA	147.246	−6.226	14.5	24.4	1.7	1.4	−0.008
KASU	146.718	−6.461	15.9	35.9	1.9	1.3	−0.034
LAE0	146.999	−6.733	29.1	53.0	2.2	1.4	−0.045
LAE1	146.993	−6.674	25.4	51.3	1.1	1.0	0.009
MADA	145.782	−5.211	23.0	36.1	1.3	1.0	0.035
MORX	147.579	−7.771	28.3	58.4	2.7	1.7	0.028
MUNG	146.715	−6.488	15.0	36.9	1.4	1.2	0.004
NADZ	146.728	−6.573	26.4	55.3	1.1	0.9	0.013
NARI	146.453	−6.347	13.0	40.1	5.1	2.8	0.051
NM31	146.227	−6.179	16.0	38.5	2.3	1.4	0.040
NM32	146.169	−6.212	27.1	48.1	2.2	1.5	0.033
NM33	146.097	−6.164	26.0	45.9	1.9	1.4	0.047
NM34	146.081	−6.148	25.8	47.0	1.7	1.3	0.012
NM35	146.091	−6.125	24.7	44.9	2.2	1.4	0.036
NM36	146.101	−6.126	24.0	44.7	2.1	1.4	0.021
OMSI	146.83	−6.673	29.6	53.4	3.1	1.6	0.022
PIND	147.513	−6.445	10.5	20.1	1.6	1.2	0.010
SAID	146.459	−5.625	19.1	32.4	2.3	1.7	0.026
SALA	147.052	−7.052	22.5	60.1	3.6	2.0	−0.024
SANG	146.321	−6.395	26.0	48.1	1.7	1.4	0.019
SASI	146.425	−6.419	21.9	48.5	4.4	2.6	0.053
SITU	147.056	−6.644	26.5	49.1	1.4	1.1	−0.003
TEPT	146.560	−5.954	12.8	32.3	3.5	2.6	0.018
TERE	146.552	−6.539	24.7	52.8	1.7	1.4	−0.016
WALI	145.459	−5.597	22.7	44.5	2.2	1.7	0.018
WANT	146.469	−6.135	11.2	33.0	1.6	1.3	0.002
WASU	147.195	−5.962	14.8	18.2	1.8	1.3	0.003
YALU	146.867	−6.602	25.2	54.3	1.2	1.0	−0.005

Table 4. Site, Location, and Velocities (ITRF2000) and 1σ Uncertainties for Sites on the Australian and Pacific Plates[a]

Site[b]	Longitude	Latitude	V_e, mm/yr	V_n, mm/yr
ALIC(A)	133.886	−23.670	32.50 ± 0.65	57.99 ± 0.55
AUCK(A)	174.934	−36.603	2.79 ± 0.57	39.63 ± 0.50
CHAT(P)	183.434	−43.956	−41.38 ± 0.57	33.30 ± 0.50
COCO(A)	96.834	−12.188	39.58 ± 1.12	47.71 ± 0.74
DARW(A)	131.133	−12.844	35.75 ± 0.88	57.53 ± 0.61
HOB2(A)	147.439	−42.805	14.51 ± 0.55	56.08 ± 0.51
KARR(A)	117.097	−20.981	39.41 ± 0.60	56.82 ± 0.54
KOKB(P)	200.335	22.126	−63.02 ± 1.07	33.24 ± 0.74
KWJ1(P)	167.730	8.722	−69.18 ± 0.64	28.30 ± 0.48
MKEA(P)	204.544	19.801	−61.44 ± 0.58	33.98 ± 0.61
NOUM(A)	166.410	−22.270	20.14 ± 0.70	45.93 ± 0.57
PERT(A)	115.885	−31.802	39.10 ± 0.41	57.01 ± 0.36
THTI(P)	210.394	−17.577	−65.27 ± 0.86	34.66 ± 0.61
TIDB(A)	148.980	−35.399	19.08 ± 0.54	56.46 ± 0.45
TOW2(A)	147.056	−19.269	29.00 ± 0.67	55.09 ± 0.57
YAR1(A)	115.347	−29.047	38.63 ± 0.39	56.53 ± 0.35

[a]The velocities at the Australian Plate sites were used to estimate an Australian Plate reference frame for the GPS velocities in Figure 3.

[b]P and A denote whether the site is on the Pacific or Australian Plate, respectively.

Table 5. Differences (East and North) Between Our ITRF2000 GPS Velocity Estimates (Table 4) and Official ITRF00 Velocities for Those Sites (ITRF2000), Difference Between Our Estimated ITRF00 Velocities and Those Estimated by *Beavan et al.* [2002] (B2002)[a]

	ITRF2000		B2002		Model[c]	
Site[b]	East	North	East	North	East	North
ALIC(A)	1.45	3.44	0.70	0.09	0.99	0.30
AUCK(A)	0.44	1.69	1.11	1.03	1.59	1.25
CHAT(P)	0.22	1.66	0.18	1.0	0.64	0.21
COCO(A)	5.17	0.43	2.52	2.19	2.76	1.75
DARW(A)	2.29	2.03	0.35	0.03	0.61	0.91
HOB2(A)	0.74	0.65	0.81	1.28	0.18	0.52
KARR(A)	0.64	3.89	0.11	0.48	0.91	0.40
KOKB(P)	1.73	0.73	0.42	0.24	0.64	1.48
KWJ1(P)	1.07	0.57	0.18	0.5	1.42	0.72
MKEA(P)	0.25	3.57	1.76	0.58	2.33	0.68
NOUM(A)	1.61	3.77	0.26	0.43	0.25	0.66
PERT(A)	0.20	0.41	0.40	0.39	0.97	0.06
THTI(P)	0.20	3.20	1.23	1.26	1.76	0.39
TIDB(A)	0.54	1.31	0.48	1.86	0.79	1.41
TOW2(A)	1.86	4.02	0.20	0.89	0.46	0.60
YAR1(A)	1.04	1.02	0.67	0.43	0.10	0.29

[a]Differences are in mm/yr.
[b]P and A denote whether the site is on the Pacific or Australian Plate, respectively.
[c]The model difference is between our ITRF00 GPS velocities and that predicted by our estimated Australian Plate and Pacific Plate poles.

frame (in our case, a fixed Australian Plate reference frame). We use 37 GPS site velocities from *Tregoning et al.* [1998, 1999] and *Tregoning* [2002] (including their site velocities from PNG and sites on the Pacific and Australian plates), 22 from *Beavan et al.* [2002], and 57 from our solution (38 site velocities from PNG and 19 from IGS sites on the Pacific and Australian plates). We do not solve for a rotation of the *Tregoning et al.* [1998] velocity field into an Australian plate reference frame, as no Australian plate velocities are provided in that paper; we instead use the Australian plate/ITRF94 pole that they estimate in order to rotate the data into an Australian Plate reference frame. Velocities from *Tregoning et al.* [1999] and *Tregoning* [2002] are in a common reference frame (ITRF97), so we combine the two data sets and solve for a single rotation. In total, we solve for the rotation of three data sets into an Australian Plate reference frame: (1) our velocities presented here, (2) *Beavan et al.*'s [2002] Australian and Pacific plate site velocities, and (3) velocities from *Tregoning et al.* [1999] and *Tregoning* [2002].

[15] We ultimately solve for Euler vectors of five tectonic blocks in the inversion: South Bismarck, Woodlark, New Guinea Highlands, North Bismarck, and Pacific plates, (Figure 1). We choose block boundaries that are consistent with geophysical and geological evidence (Figures 1 and 4). Previous studies by *Tregoning et al.* [1998, 1999] and *Tregoning* [2002] used GPS data to estimate Euler poles for the South Bismarck, North Bismarck, and Woodlark microplates. We utilize additional GPS data from the South Bismarck, Woodlark, and New Guinea Highlands tectonic blocks and earthquake slip vectors bounding all of the microplates to produce a regional, kinematically consistent model for PNG microplate tectonics. Unlike previous studies, we also account for the effect of elastic strain on GPS sites in the PNG region when estimating Euler vectors for the tectonic blocks.

[16] We solve for coupling on several faults in the region: the Ramu-Markham Fault, Owen Stanley Fault Zone, Bismarck Sea Seismic Lineation, and Highlands Fold and Thrust Belt. We assume a ramp-detachment geometry for the Ramu-Markham Fault, consistent with previous geophysical

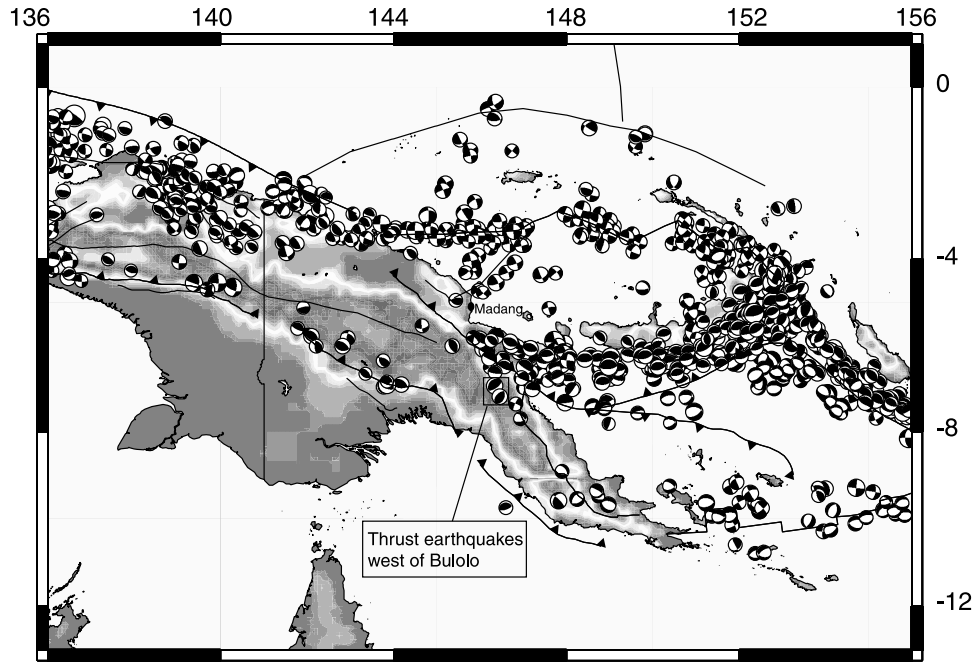

Figure 4. Shallow seismicity (0–40 km) for the last 25 years. Focal mechanisms from the Harvard CMT catalogue [*Dziewonski and Woodhouse*, 1983]. Small box shows focal mechanisms for earthquakes near Bulolo discussed in the text. See color version of this figure in the HTML.

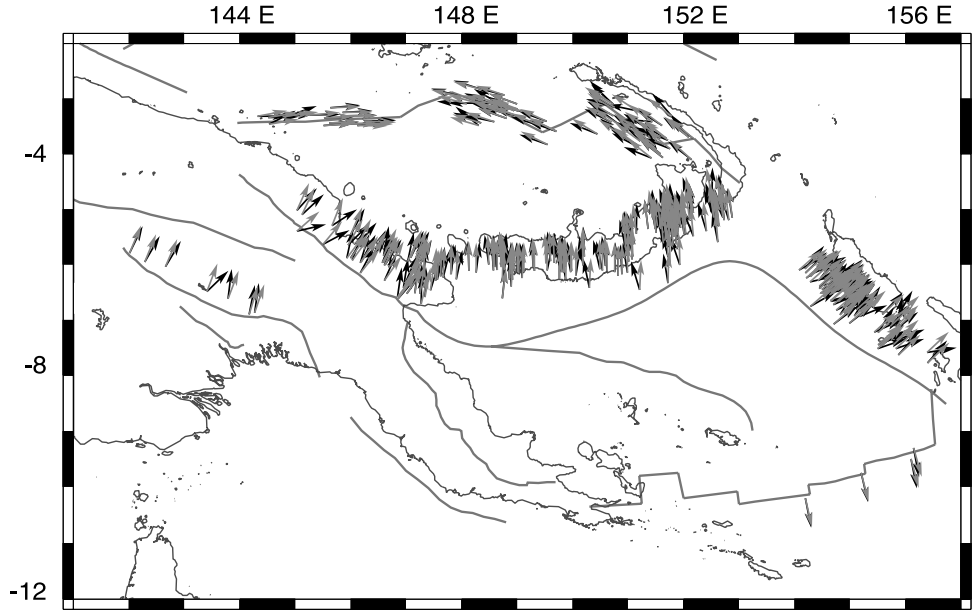

Figure 5. Observed (black) and calculated (red) earthquake slip vector azimuths and transform orientations from best fit model. See color version of this figure in the HTML.

and geological studies [*Abbott*, 1993; *Abers and McCaffrey*, 1994; *Stevens et al.*, 1998]. The Ramu-Markham Fault extends to 40 km depth in the model. Locking beyond this depth is unlikely, so we force the deepest part of the fault to have zero coupling. To smooth the locking model, locking values at fault nodes with large uncertainties are forced to equal values at adjacent nodes. The GPS data required extensive locking on the Ramu-Markham Fault in all of the model runs that we discuss below (Figure 6). The data also require strain accumulation on the Owen Stanley Fault Zone and the Bismarck Sea Seismic Lineation. Data are insufficient near the Highlands Fold and Thrust Belt Faults to resolve the locking distribution there.

[17] At first, we experimented with a five-block model (Australia, South Bismarck, Woodlark, North Bismarck, Pacific). As the sites in the New Guinea Highlands deviate significantly from Australian plate motion, we initially considered all sites north of the Woodlark spreading center and the New Guinea Highlands Fold and Thrust Belt and to the south of the Ramu-Markham Fault and New Britain Trench to be on a single block (the Woodlark Block). This produced a $\chi^2_n = 2.6$ and did not match velocities of three GPS sites in the Woodlark basin (GUA1, LOUS, and SALA), nor earthquake slip vectors on the New Britain Trench. In this model, predicted velocities in the Woodlark Basin were ~20 mm/yr too slow compared to GPS-derived velocities. East of 147.5°E, most earthquake slip vectors on the New Britain Trench are oriented N–S to NNW, but the five-block model returned slip vectors with a more northeasterly orientation east of 147.5°E (Figure 7).

[18] Our preferred model comprises six tectonic blocks (Australia, South Bismarck, Woodlark, North Bismarck, New Guinea Highlands, and Pacific), with large locked patches on the Ramu-Markham Fault ($\chi^2_n = 1.99$) (Figure 6). This run required 44 free parameters (5 block rotation vectors, Euler vectors to rotate 3 GPS data sets into an Australia-fixed reference frame, and locking at 20 free nodes on faults in the region). We call the additional block the New Guinea Highlands Block, since it likely encompasses much of the Highlands (Figures 1 and 3). Our best fit poles of rotation (Figure 8) are compared to poles obtained from other studies in Table 6.

[19] We used an F test to determine if the addition of the Highlands Block gives a statistically significant improvement to the data fits. Comparison of the case of an independent Highlands Block ($\chi^2_n = 1.99$, 565 data, 44 free parameters) to the case where it is attached to the Woodlark Plate ($\chi^2_n = 2.60$, 565 data, 41 free parameters) yields a low probability (5.2×10^{-4}) that random chance has caused this improvement in fit to the data. Thus the addition of a separate New Guinea Highlands Block is strongly supported by the data.

5.1. Implications of This Model for Motion at Active Plate Boundaries in PNG

[20] Expected relative motions across plate boundaries in PNG based on the best fit model are shown in Figure 9. Predicted motion at the Ramu-Markham Fault shows convergence normal to the fault trace, in good agreement with other studies [*Abers and McCaffrey*, 1994; *Stevens et al.*, 1998; *Tregoning et al.*, 1998, 1999]. Our tectonic model predicts that motion across the Ramu-Markham Fault increases from a few mm/yr in the northwest (at ~144.5°E) to 61 mm/yr at 147.2°E (Figure 9). Convergent deformation west of 145.5°E may be taken up either on the Ramu-Markham Fault or on the Adelbert Range front or on a combination of the two. Convergence on the Ramu-Markham fault system probably ends near 144.5°E, just northwest of the terminus of the topographic high colinear with the Finisterre Range uplift (Figure 1). If the Ramu-Markham Fault or related faults west of 144.5°E accommodate any Highlands-South Bismarck motion, extension would be expected on these structures, based on the location of the Highlands-South Bismarck Euler pole. No clear

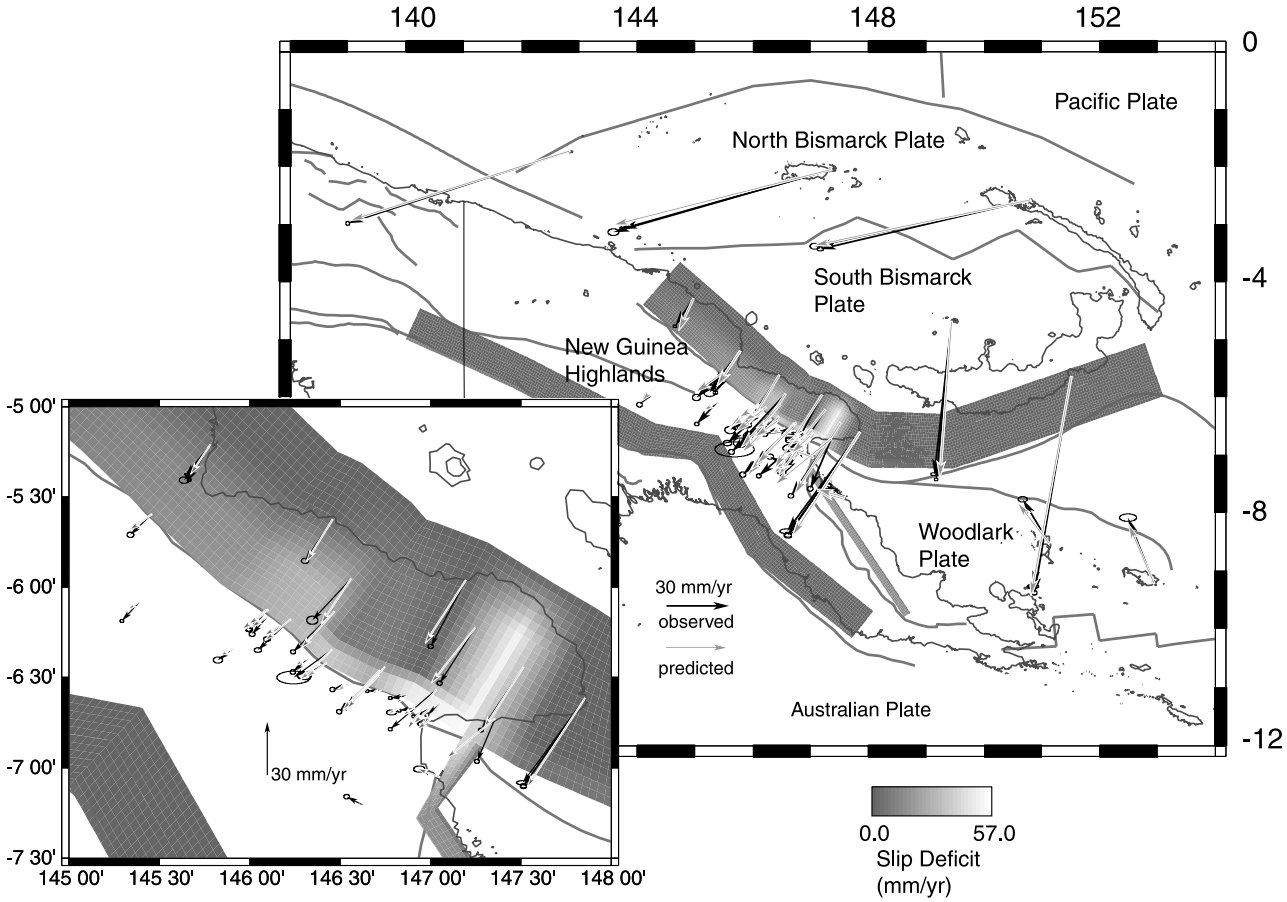

Figure 6. Fits and plate coupling from the best fit, six-block model. Predicted GPS velocities are based on the best fit model, while the black vectors are the observed GPS velocities. Shading shows the distribution of slip deficit rate on the Ramu-Markham Fault. Beneath the central Huon Peninsula (between 6 and 6.5°S and 147–147.5°E, the slip deficit reaches 57.0 mm/yr). Northeast of the Kaiapit network (near 6°S and 145°E), the slip deficit is as high as 30 mm/yr. Inset shows an expanded view of the Ramu-Markham Fault region. Where the faults are far away from any GPS sites (e.g., Highlands Fold and Thrust Belt and the eastern New Britain Trench), coupling on the faults is unconstrained. See color version of this figure in the HTML.

evidence supports or contradicts extension NW of the termination of the Finisterre topographic high.

[21] In line with previous studies [*Tregoning et al.*, 1998, 1999], our tectonic model predicts that convergence along the New Britain Trench should increase from 55 mm/yr at 147.5°E to ~130 mm/yr at 151.5°E. In calculating the relative motions here, we assume that what has been called the Solomon Sea Plate (i.e., the area between the Trobriand Trough and the New Britain Trench) is part of the Woodlark Plate. Whether or not the Trobriand Trough is accommodating significant active deformation has been a subject of some debate [*Cooper and Taylor*, 1987; *Abers and Roecker*, 1991; *Kirchoff-Stein*, 1992; *Pegler et al.*, 1995]. We cannot answer this question using GPS methods as there is no subaerial landmass on what would be the Solomon Sea Plate. Therefore it must be understood that if the Solomon Sea Plate is independent of the Woodlark Plate, our estimate of relative motions at the New Britain Trench in Figure 9 would be slightly different.

[22] Seismological and geological evidence for activity in the Highlands is focused in the southern Highlands Fold and Thrust Belt, well to the south of our southernmost Highlands GPS sites (HAGE, GOKA, and AIYU). Thus we assume in our kinematic model that Highlands/Australia relative motion is accommodated on faults in the Highlands Fold and Thrust Belt. According to our model, convergence occurs at an azimuth roughly normal to the northwest striking fold and thrust belt structures. We predict around 14 mm/yr of convergence at 142°E on the fold and thrust belt, decreasing to slow convergence (<2 mm/yr) at 145°E (Figure 9). This is comparable to rates from *Abers and McCaffrey* [1988] using seismic moment rates and crustal thickening estimates from the Fold and Thrust Belt. Approximately 10 mm/yr of convergence may occur across the New Guinea Highlands Fold and Thrust Belt in the region of a M_w = 6.6 earthquake that occurred in March 2000. It is also possible that some of the convergence between the Highlands and Australia is accommodated on structures north of the fold and thrust belt but south of our sites GOKA and HAGE.

[23] If the northern end of the Owen Stanley Fault Zone (i.e., north of 8°S) is the primary Woodlark/Highlands

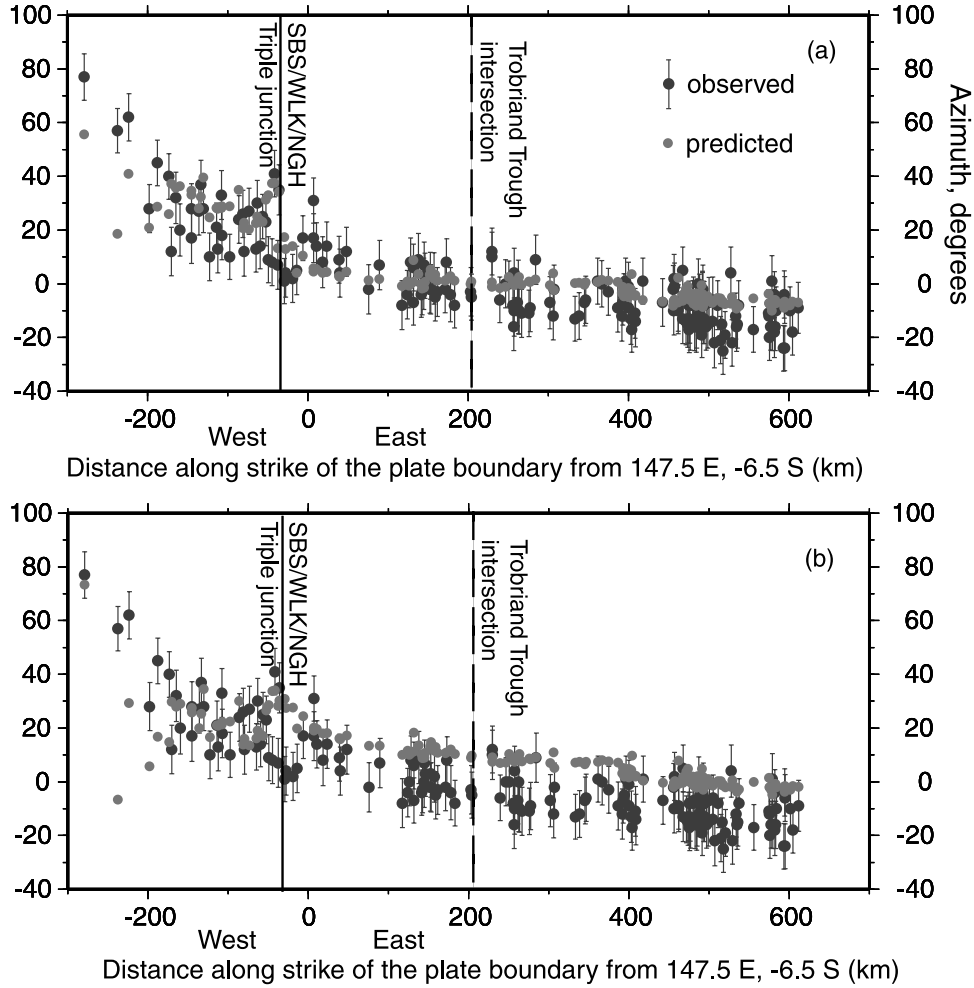

Figure 7. Observed and calculated earthquake slip directions along the Ramu-Markham Fault and New Britain Trench. The *x* axis is distance in kilometers along strike of the plate boundary to the east and west of the triple junction with the South Bismarck, New Guinea Highlands and Woodlark Plates. The red data points are the observed slip vectors (with ten degree error bars), while the green points are based on the best fit model. Figure 7a assumes that the New Guinea Highlands and Woodlark Plates rotate independently of one another. Figure 7b assumes that the New Guinea Highlands and Woodlark rotate about the same pole. Note that the data are fit better when the New Guinea Highlands is assumed to be separate from Woodlark. See color version of this figure in the HTML.

boundary, we predict 20 mm/yr of convergence perpendicular to the Owen Stanley Fault Zone north of 8°S. This convergent deformation north of 8 S may be taken up via folding in the Aure Trough, shortening on north-south trending faults west of Bulolo, and activity on the Owen Stanley fault zone (Figure 1). Broadly folded Quaternary sediments in the Aure Trough agree with recent shortening between the New Guinea Highlands and the Papuan Peninsula [*Dow*, 1977]. A series of M_w 6.4–5.5 thrust earthquakes occurred near 6.8°S, 146.4°E in June 2001, ~30 km to the north of the site BULO (Figure 4). They were either east or west dipping thrust events, also consistent with east-west oriented compression between the Woodlark and Highlands Plates in this region. These events were west of our inferred Highlands/Woodlark boundary and west of the main faults in the Owen Stanley fault zone. Therefore it is possible that there are multiple independent small-scale blocks in the boundary zone between the Highlands and Woodlark Plates on the Papuan Peninsula, generating a more complex tectonic block interaction than we can resolve with existing GPS data, or that the shortening between the Highlands and the Papuan Peninsula is accommodated on multiple structures. For example, the site BULO appears to be moving northwest at 10 mm/yr relative to Australia, while our plate motion model predicts that BULO should move to the southwest at a few millimeters per year if it is on the Highlands Plate. We propose that most of the Highlands/Woodlark relative motion is taken up along a fault zone that projects into the New Britain Trench/Ramu-Markham Fault near 147.5°E, on the basis of a change in orientation of earthquake slip vectors at the New Britain Trench/Ramu-Markham Fault near 147.5°E (discussed later) and the fact that the GPS velocities in the Lae area are consistent with Highlands Block motion, while SALA appears to be on the Woodlark Plate.

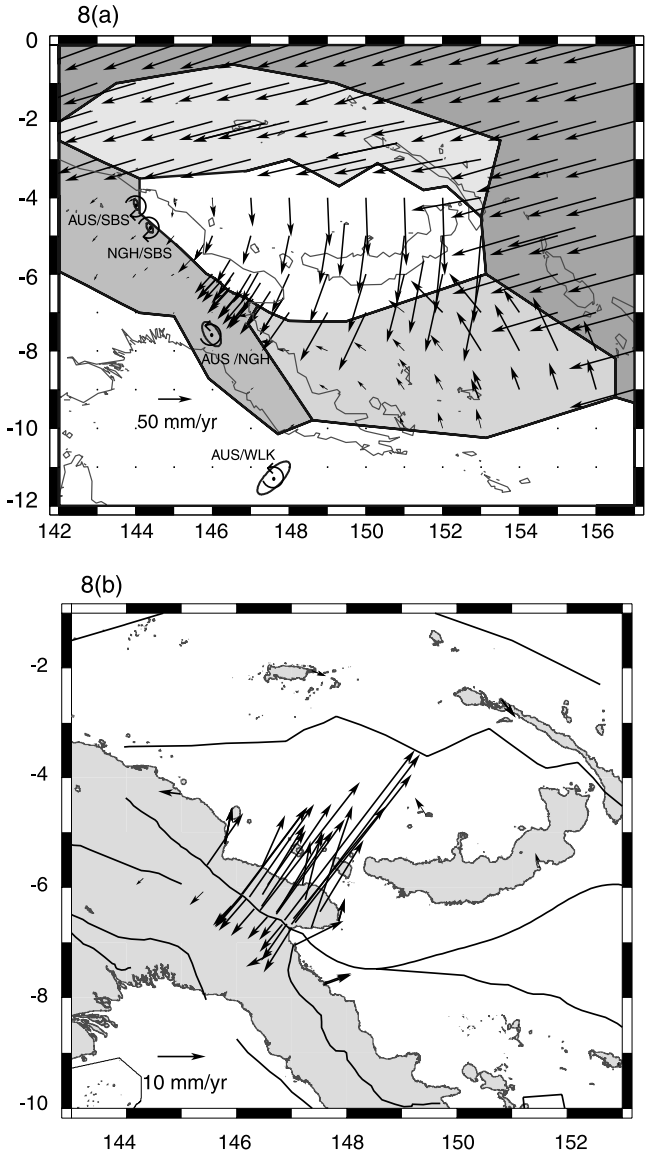

Figure 8. (a) The rotational part of the velocity field in PNG (relative to Australia) as predicted by the Euler vectors of the best fit model. Also shown is a selection of the poles of rotation (and error ellipses) from the best fit model. The poles of rotation locations are labeled based on which plate pair they correspond to. For example, the pole of rotation for the New Guinea Highlands relative to Australia is labeled AUS/NGH. NGH, New Guinea Highlands; AUS, Australia; SBS, South Bismarck; and WLK, Woodlark. (b) Velocities due to elastic strain. The elastic strain is mostly due to locking on the Ramu-Markham Fault, although locking on the Bismarck Sea Seismic Lineation and the Owen Stanley Fault Zone also influences the GPS site velocities.

[24] Our estimate of the Woodlark/Australia Euler vector is based on three GPS velocities from *Tregoning et al.* [1998] (GUA1, LOUS, and MORO), two site velocities from our network (MORX and SALA), 224 earthquake slip vectors on the New Britain Trench, and four transform orientations on the Woodlark spreading center [*Goodliffe et al.*, 1997; *Taylor et al.*, 1999]. Our calculated Woodlark/Australia Euler vector predicts spreading on the Woodlark spreading center in a direction perpendicular to the ridge that increases from ~12 mm/yr at 149.2°E (on the Papuan Peninsula in the subaerial portion of the rift) to 42 mm/yr at 155.25°E (Figure 9). This is ~30% slower than rates deduced from magnetic lineations from the Brunhes chron [*Taylor et al.*, 1995] but slightly faster than those predicted by previous GPS studies [*Tregoning et al.*, 1998]. The pole location that we obtain for the Woodlark Plate (relative to Australia) is closer to PNG and 2.4° to the east of that obtained by *Tregoning et al.* [1998]. Our Woodlark/Australia pole agrees well with normal faulting earthquakes associated with Woodlark Basin opening at least as far west as 148°E [*Abers et al.*, 1997]. It is probable that faults in the southern Papuan Peninsula are accommodating some Woodlark/Australia relative motion. From approximately 9.5°S to 8.5°S, we predict 10–15 mm/yr of left-lateral strike-slip motion, gradually changing to convergent deformation perpendicular to the Owen Stanley fault zone (Figure 9). Left-lateral shear in the southern part of the fault zone is consistent with geological evidence for NW–SE striking, recently active left-lateral faults there [*Davies*, 1971]. We do not know whether this deformation is distributed among several faults or localized onto one or two main faults in the Papuan Peninsula.

[25] We find rapid rates of motion on the Bismarck Sea Seismic Lineation, also in agreement with previous studies. We predict ~110 mm/yr of motion parallel to the western portion of the Bismarck Sea Seismic Lineation, and ~140 mm/yr of motion on the eastern end of the Bismarck Sea Seismic Lineation (Figure 9). This is taken up by a combination of strike-slip faulting and the opening of the Manus and New Guinea basins. If the Manus Trench (Figure 1) is the primary boundary with North Bismarck and Pacific Plates, we expect very slow rates of convergence in the western section (5 mm/yr), increasing to 12 mm/yr of convergence near 152°E (Figure 9). These rates are similar to those predicted by *Tregoning* [2002]. However, we use more data than *Tregoning* [2002] to constrain North Bismarck Plate motion (58 earthquake slip vectors on the Bismarck Sea Seismic Lineation), and we estimate locking on the Bismarck Sea Seismic Lineation, which affects all three of the GPS sites on the North Bismarck Plate and consequently influences the North Bismarck Euler vector estimated.

5.2. Are These Blocks Rigid?

[26] Continental deformation is sometimes characterized by diffuse permanent deformation over broad regions [e.g., *Isacks et al.*, 1968; *Molnar and Tapponier*, 1975; *McKenzie and Jackson*, 1983; *Molnar*, 1988]; in the extreme, some consider this as continuous deformation [e.g., *England and McKenzie*, 1982; *Vilotte et al.*, 1982; *Houseman and England*, 1986]. The New Guinea Highlands are a fine example of continental orogenesis, so can the Highlands truly be approximated as a rotating elastic block? Velocities from GPS sites in the Highlands fit a rigid block model well, with an RMS of 3.5 mm/yr (Figure 6). Additionally, shallow seismicity in the Highlands (<30 km deep) is focused on faults in the fold and thrust belt in the southern Highlands, well to the south of our Highlands GPS sites (Figure 4). Geological evidence also indicates concentrated

Table 6. Euler Vectors for the Microplates Discussed in This Study Relative to the Australian Plate and Selected Adjacent Microplates[a]

Plate Pair[b]	Latitude	Longitude	Rate, deg/Myr	e_{max}	e_{min}	Azimuth	Source
ITRF00-AUS	32.00	39.13	0.621 ± 0.003	0.59	0.33	163	this study
ITRF00-AUS	32.76	37.54	0.621±0.002	0.40	0.13	109	*Beavan et al.* [2002]
AUS-PAC	−61.08	184.48	1.079 ± 0.003	0.20	0.16	325	this study
AUS-PAC	−61.04	184.19	1.078 ± 0.004	0.37	0.17	82	*Beavan et al.* [2002]
AUS-WLK	−11.28	147.6	2.82 ± 0.18	0.55	0.21	44	this study
AUS-WLK	−10.8	145.2	1.86 ± 0.03	2.01	1.58	74	*Tregoning et al.* [1998]
AUS-WLK	−12	144	2.44	NA	NA	NA	*Taylor et al.* [1999]
AUS-WLK	−9.5	148.93	5.60	NA	NA	NA	*Benes et al.* [1994]
AUS-SBS	−4.18	144.02	−7.45 ± 0.13	0.14	0.05	−18	this study
AUS-SBS	−4.36	144.54	−7.91 ± 0.33	0.24	0.16	281	*Tregoning et al.* [1999]
AUS-NGH	−7.56	145.98	1.63 ± 0.20	0.36	0.18	148	this study
AUS-NBS	−51.3	165.31	1.25 ± 0.06	4.71	0.35	113	this study
AUS-NBS	−50.6	166.7	1.23 ± 0.07	4.1	0.4	37	*Tregoning* [2002]
PAC-NBS	−5.54	134.71	.34 ± 0.09	5.24	1.46	−165	this study
PAC-WLK	9.45	139.98	2.39 ± 0.17	2.17	0.23	−55	this study
NGH-SBS	−4.79	144.36	−9.07 ± 0.24	0.14	0.07	−27	this study
WLK-SBS	−6.13	144.98	−10.25 ± 0.22	0.20	0.074	170	this study
NGH-WLK	−16.31	149.86	1.20 ± 0.26	3.0	1.1	101	this study

[a]In all cases, Euler vectors are for the second plate relative to the first; e_{max}, e_{min}, and azimuth refer to the maximum and minimum uncertainties of the error ellipse and the azimuth of the major axis, respectively. Positive rotation rates indicate anticlockwise motion. NA, not available.
[b]AUS, Australian Plate; PAC, Pacific Plate; WLK, Woodlark Plate; NGH, New Guinea Highlands Block; SBS, South Bismarck Plate; NBS, North Bismarck Plate.

deformation in the fold and thrust belt of the southern Highlands [*Hamilton*, 1979; *Hill and Gleadow*, 1989; *Hill*, 1991]. We suggest that the central part of the Highlands is rotating as an elastic block, while the deformation at the edges of the block may be taken up diffusely among several faults in the southern New Guinea Highlands Fold and Thrust Belt. Whether or not the Highlands Block continues westward into western PNG and Irian Jaya is unclear.

[27] The Highlands boundary with the South Bismarck Plate is at the Ramu-Markham Fault in the north, and the

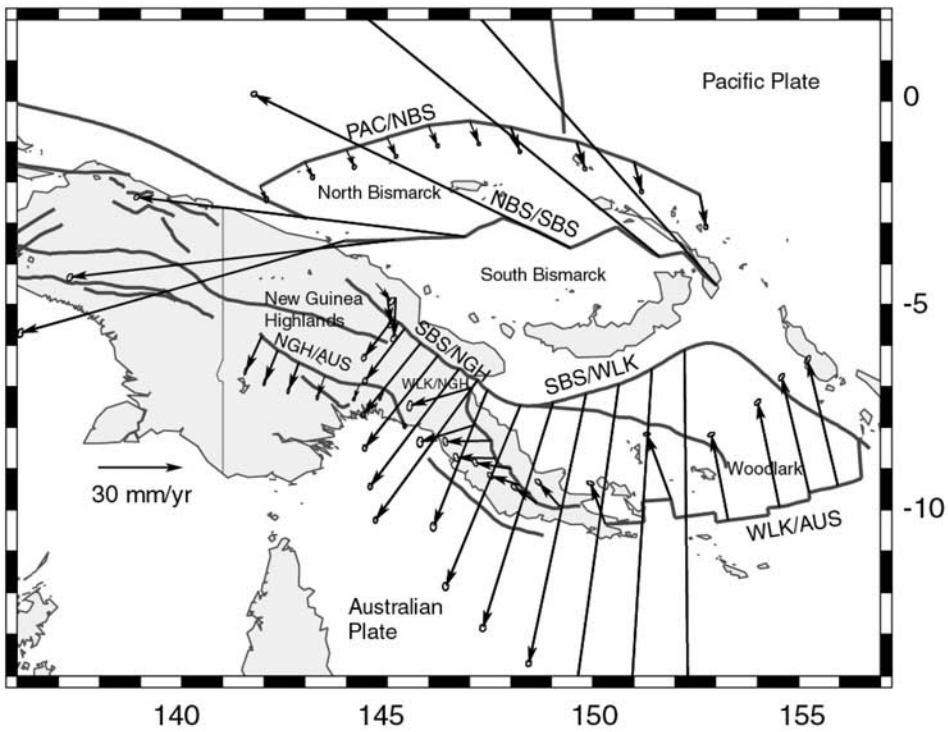

Figure 9. Predicted relative motions across block boundaries from the best fit model. Euler vectors between the various blocks are used to obtain these estimates. At each boundary we have labeled the two plates involved. For example, we have the Ramu-Markham Fault labeled "SBS/NGH," which means the relative motion shown there is the South Bismarck Plate relative to a fixed New Guinea Highlands Plate. AUS, Australian Plate; PAC, Pacific Plate; WLK, Woodlark Plate; NGH, New Guinea Highlands Block; SBS, South Bismarck Plate; NBS, North Bismarck Plate. See color version of this figure in the HTML.

southern boundary with Australia is likely the fold and thrust belt in the southern Highlands. The eastern boundary of the Highlands Block with the Woodlark microplate is probably a broad zone in the Papuan Peninsula, as discussed previously. The velocities on the Woodlark Plate fit a rigid plate model well. The residual strain rate (estimated from residuals of the GPS site velocities to the best fit model) of the Woodlark Plate is relatively small, 30–50 nstrain/yr.

[28] The South Bismarck Plate appears to be a rigid microplate, in agreement with *Tregoning et al.* [1999]. We can fit the data on and at the edges of the South Bismarck Plate adequately using a combination of rigid block rotation and elastic strain due to locking on the New Britain Trench/Ramu-Markham Fault. The exception to this is the velocity of the site BUKA (Figure 6); we speculate that an out-of-sequence thrust mapped to the north of that site [*Abbott*, 1993; *Abbott et al.*, 1994b] is accommodating some South Bismarck/Woodlark relative motion. Using the velocity residuals, we find the residual strain rate in the South Bismarck Plate to be quite small, only 5–15 nstrain/yr. Previous workers have speculated that active strike slip faults run perpendicular to the Ramu-Markham Fault in the Finisterre Collision [*Abbott et al.*, 1994b; *Abers and McCaffrey*, 1994]. The relatively low level of internal deformation within the South Bismarck microplate implies that these cross faults accommodate little, if any, deformation. Moreover, paleomagnetic declinations indicate that the Finisterre terrane has been rotating as a single entity at ~8°/Myr for the last 4 Myr [*Falvey and Pritchard*, 1982; *Weiler and Coe*, 2000], agreeing well with instantaneous geodetic estimates of South Bismarck Plate rotation.

6. Earthquake Slip Vectors and Activity on the Trobriand Trough

[29] Addition of a separate New Guinea Highlands Block to the tectonic model yields a good fit to earthquake slip vectors on the Ramu-Markham Fault and New Britain Trench (Figures 5 and 7). *Abers and McCaffrey* [1994] noted an ~20–30° rotation of earthquake slip vector orientations near 148°E. They ascribed this change in slip vector orientation to deformation of the upper plate (Finisterre Range), but the GPS data do not support this explanation. *Pegler et al.* [1995] suggested that the change in slip vector orientation is due to faulting in the footwall, that is, the subduction of two different plates (the Australian and Solomon Sea Plates). *Tregoning and McQueen* [2001] infer that the change in slip vector orientation is gradual between 147°E and 148°E. However, by plotting the slip vectors with respect to distance along strike of the Ramu-Markham Fault/New Britain Trench Plate boundary, rather than by longitude as *Tregoning and McQueen* [2001] did, the change appears to be abrupt near 147°E, not gradual (Figure 7). This slip vector orientation change occurs at least 200 km west of where the Trobriand Trough intersects the New Britain Trench. (Figure 7). Furthermore, there appears to be no change in slip vector orientation where the Trobriand Trough intersects the New Britain Trench (near 148.5°E), arguing against both significant activity on the Trobriand Trough, and a separate Solomon Sea microplate (Figure 7).

[30] We suggest instead that the abrupt orientation change in slip vectors on the New Britain Trench/Ramu-Markham Fault marks the intersection of the triple junction between the Woodlark, New Guinea Highlands, and South Bismarck microplates. Where the Ramu-Markham Fault separates the South Bismarck and Highlands Plates, our predicted slip vectors are oriented NE, due to the relative motion between those two plates (Figures 5 and 7). Likewise, where the Ramu-Markham Fault and New Britain Trench bound the South Bismarck and Woodlark Plates, slip vectors are dominantly oriented N-S. Close examination indicates that this azimuth change from northeast to north-south may occur as far west as 147°E (Figure 7). We suggest the primary boundary between the Highlands and Woodlark Plates is along the Owen Stanley Fault Zone, and projects to the Ramu-Markham Fault/New Britain Trench at 147.5°E. Our inferred western boundary of the Woodlark Plate is ~60 km farther to the east than *Tregoning et al.*'s [1998] on the basis of evidence from the earthquake slip vector orientations, the Highlands-like motion of the GPS sites in the Lae area, and that the velocity at site SALA fits Woodlark Plate motion.

[31] We tested whether or not the earthquake slip vectors on the New Britain Trench show that the Solomon Sea Plate moves independently of the Woodlark Plate by including a Solomon Block in our kinematic model. The Euler vector we calculate for a Solomon Block is statistically indistinguishable from the Euler vector we obtain for Woodlark. However, when we add to the data set a slip vector from a M_w 7.2 northeast striking, right-lateral, strike-slip event near 154.2°E, 8.4°S at 7.9 km depth [*Abers et al.*, 1997], assuming that this event represents Solomon Sea/Woodlark relative motion, we obtain a pole of rotation for the Solomon Sea Plate that predicts extension on the Trobriand Trough. However, very little is known about the fault that generated this earthquake, so we can't be sure that it does represent Solomon Sea/Woodlark Plate relative motion. Seismic reflection data gathered across the Trobriand Trough identified normal faults in this region [*Soto-Cordero*, 1998], which are consistent with our suggestion that extension, rather than convergence currently occurs at the Trobriand Trough. At present, the data are insufficient to clearly demonstrate a separate Solomon Sea Plate, but neither can we rule it out.

7. Mechanics of Microplate Rotation in New Guinea

[32] The New Guinea Highlands and Woodlark Plates rotate anticlockwise relative to Australia, consistent with the left-lateral sense of shear between the Australian and Pacific Plates (although shear is not necessarily the cause of these rotations). The Bird's Head Block in western New Guinea also rotates counterclockwise about a nearby pole [*Stevens et al.*, 2002]. The South Bismarck Plate is rotating clockwise, which is inconsistent with being driven by left-lateral megashear between the Pacific and Australian Plates. What drives the extremely rapid (7.8°/Myr) clockwise rotation of the South Bismarck Plate?

[33] The Highlands/South Bismarck pole (4.8°S, 144.4°E) is near the Highlands/South Bismarck Plate boundary, close to the western terminus of the high topography of the Finisterre Range uplift (Figures 1 and 8). Because of its thick, buoyant crust, the Highlands litho-

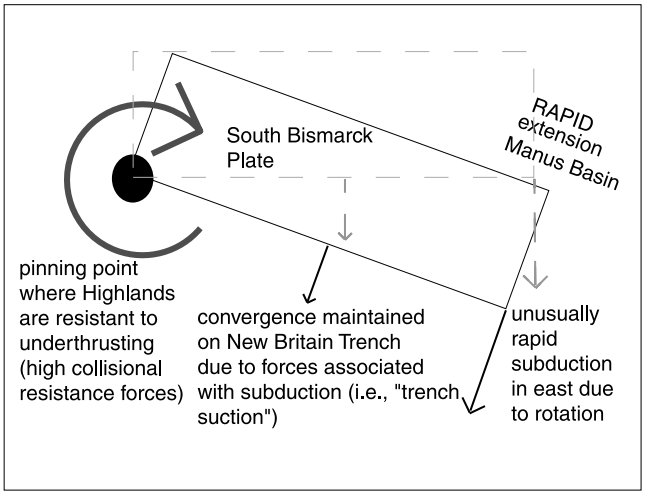

Figure 10. Schematic of the collision-induced microplate rotation model explaining the rotation of the South Bismarck Plate. See color version of this figure in the HTML.

sphere resists subduction below the South Bismarck Plate. Such buoyancy forces have been termed "colliding resistance" forces [*Forsyth and Uyeda*, 1975] and inhibit motion between the Highlands and South Bismarck Plates. Conversely, "trench suction" forces [*Elsasser*, 1971; *Forsyth and Uyeda*, 1975; *Chapple and Tullis*, 1977; *Chase*, 1978] are acting at the South Bismarck/Woodlark plate boundary where subduction at the New Britain Trench is ongoing. This force drives the South Bismarck Plate toward the lower plate. These "collisional resistance" and "trench suction" forces are each classified as plate edge forces [*Forsyth and Uyeda*, 1975; *Chapple and Tullis*, 1977], as they are normal forces exerted across the plate boundary. This change from collision to subduction along the southern boundary of the South Bismarck Plate exerts a torque on the plate, causing it to rotate rapidly with respect to the lower plate (i.e., the New Guinea Highlands) about an Euler pole where the "collisional resistance" forces slow the convergence to zero (Figures 8 and 10). Hence the manner in which plate boundary forces are balanced between the Highlands, South Bismarck, and Woodlark Plates and the rates of convergence they allow drives the rapid clockwise rotation of the South Bismarck Plate relative to the rest of New Guinea. The initiation of the Finisterre Collision established this gradient in convergence rates along the southern South Bismarck Plate boundary. We therefore suggest that the rapid clockwise rotation of the South Bismarck Plate is a direct consequence of the collision. Similar mechanisms for microplate rotation and subsequent back-arc opening (invoking a variation in boundary conditions along convergent margin boundaries) have been suggested for the North Island of New Zealand [*Reyners*, 1998], Okinawa [*Viallon et al.*, 1986], and the Tonga-New Hebrides region [*Pelletier et al.*, 1998; *Ruellan et al.*, 2003; *Calmant et al.*, 2003].

[34] This collision-induced rapid rotation of the South Bismarck Plate has also influenced the regional tectonics. The Finisterre Collision initiated at 3.5–4 Ma [*Abbott et al.*, 1994a], and rapid spreading (60–140 mm/yr, full spreading rates) in the Manus and New Guinea basins (Figure 1) initiated around 3.5 Ma [*Taylor*, 1979]. The clockwise rotation of the South Bismarck Plate has caused rapid divergence between the Pacific and South Bismarck Plates along the Bismarck Sea Seismic Lineation, opening the Manus and New Guinea basins [*Taylor*, 1979]. We suggest that this back-arc basin formed due to rapid rotation of the South Bismarck Plate away from the Pacific Plate as a consequence of the changes in the balance between collision and subduction forces along the Ramu-Markham Fault and New Britain Trench (Figure 10). Hence the opening of the Manus and New Guinea back-arc basins is driven in part by the Finisterre Collision itself, and is not solely a consequence of subduction.

[35] Previous workers have suggested that the counterclockwise rotation of the Woodlark Plate is controlled by left-lateral shear between the Pacific and Australian Plates and that the Woodlark Plate behaves as an edge-driven roller bearing [*Hamilton*, 1979; *Schouten and Benes*, 1993]. However, our current work does not support the edge-driven roller-bearing hypothesis for the Woodlark Plate. The relative poles of rotation for microplates (relative to the surrounding plates) in a roller-bearing situation would fall on the plate boundaries [*Schouten et al.*, 1993]. However, the location of the Pacific/Woodlark pole a few thousand kilometers from the Woodlark/Pacific plate boundary (Table 6) contradicts the roller bearing hypothesis for Woodlark Basin opening. The Australia/Woodlark Euler pole is close to the Australia/Woodlark plate boundary (Figure 8). In contrast, if basal shear is driving Woodlark rotation, then we would expect this Euler vector to occur further to the south, well within the Australian Plate, following the model of *McKenzie and Jackson* [1983, 1986] for basally driven block rotations. Forces associated with rapid subduction at the New Britain and San Cristobal Trenches (e.g., slab pull) likely have a more important influence on the motion of the Woodlark Plate [*Weissel et al.*, 1982].

[36] It is unclear what is driving the New Guinea Highlands Block rotation. The Highlands/Australia pole is located near the boundary with the Highlands and Australian Plates, not within the bounding Australian Plate, which rules out the likelihood that basal shear forces are driving Highlands rotation. It is plausible that the current deformation in the Highlands Fold and Thrust Belt is somehow a consequence of the Finisterre Collision to the north. Because of the similarity between the New Guinea Highlands and Woodlark microplate kinematics, it is also possible that Highlands rotation is related to Woodlark opening, though how this occurs is uncertain.

8. Summary of Major Conclusions

[37] We present a new active tectonic model for Papua New Guinea that requires the existence of six separate tectonic blocks, including a previously unrecognized New Guinea Highlands Block. In agreement with previous studies, the major active plate boundaries in PNG correspond with the Ramu-Markham Fault, New Britain Trench, Woodlark spreading center, the Bismarck Sea Seismic Lineation, and the Owen Stanley Fault Zone. We see no evidence for significant activity on the Trobriand Trough, based on a lack of change in orientation of earthquake slip vectors where the Trobriand Trough intersects the New Britain Trench. The New Guinea Highlands Fold and Thrust Belt is probably

accommodating up to 15 mm/yr of convergence between the New Guinea Highlands and Australian Plates. GPS observations reveal extensive locking along the Ramu-Markham Fault, the location of an active arc-continent collision in northern PNG. Locking also occurs on the Bismarck Sea Seismic Lineation and the Owen Stanley Fault Zone. Locking on the fold and thrust belt faults is unresolvable due to a lack of nearby data. Most GPS sites in PNG are affected by elastic strain to some degree (Figure 8).

[38] We suggest that the onset of the Finisterre Collision initiated the rapid rotation of the South Bismarck Plate. Rotation occurs because of the necessity to balance resistance to convergence at the collision zone, and the forces driving convergence on the subduction zone to the east. As suggested by previous workers, Woodlark Plate rotation is most likely dominated by slab-pull forces associated with subduction at the New Britain and San Cristobal Trenches [e.g., *Weissel et al.*, 1982]. Although PNG straddles the Pacific/Australia boundary where extremely rapid shear occurs, microplate kinematics in PNG are dominated by a combination of plate boundary forces induced by collision and subduction, rather than by forces associated with shear across the plate boundary zone.

[39] **Acknowledgments.** Comments on an earlier version of this paper by John Beavan, Susan Ellis, and Martin Reyners are greatly appreciated. Thorough reviews by Geoff Abers (Associate Editor), Paul Tregoning, and an anonymous reviewer improved the manuscript substantially. Mark Murray provided advice on the GPS data analysis. Discussions with Lon Abbott, Hugh Davies, Bob Findlay, Andrew Goodliffe, and Peter Weiler were valuable. We thank Rod Little and Russell Jackson for their support and assistance in PNG. Fieldwork assistance given to us by many students and staff of the Surveying and Lands Department, University of Technology, Lae, PNG, was vital to the success of this project. In particular, thanks to the many citizens of Papua New Guinea who showed us their generous hospitality during the course of this work. Support for the work came from NSF grants EAR-9728749 and OCE-9907153 to Silver and EAR-9114349 to McCaffrey. Wallace acknowledges support from a NASA fellowship.

References

Abbott, L. D. (1993), Structural and sedimentological history of a progressive arc-continent collision: The Finisterre Range, northern Papua New Guinea, Ph.D. thesis, Univ. of Calif., Santa Cruz.

Abbott, L. D., E. A. Silver, P. R. Thompson, M. V. Filewicz, C. Schneider, and Abdoerrias (1994a), Stratigraphic constraints on the development and timing of arc-continent collision in northern Papua New Guinea, *J. Sediment. Res.*, *Sect. B*, *64*, 169–183.

Abbott, L. D., E. A. Silver, and J. Galewsky (1994b), Structural evolution of a modern arc-continent collision in Papua New Guinea, *Tectonics*, *13*, 1007–1034.

Abers, G. (1989), Active tectonics and seismicity of New Guinea, Ph.D. thesis, Mass. Inst. of Technol., Cambridge.

Abers, G., and R. McCaffrey (1988), Active deformation in the New Guinea fold-and-thrust belt: Seismological evidence for strike-slip faulting and basement-involved thrusting, *J. Geophys. Res.*, *93*, 13,332–13,354.

Abers, G. A., and R. McCaffrey (1994), Active arc-continent collision: Earthquakes, gravity anomalies, and fault kinematics in the Huon-Finisterre Collision zone, Papua New Guinea, *Tectonics*, *13*, 227–245.

Abers, G. A., and S. W. Roecker (1991), Deep structure of an arc-continent collision: Earthquake relocation and inversion for upper mantle P and S wave velocities beneath Papua New Guinea, *J. Geophys. Res.*, *96*, 6379–6401.

Abers, G. A., C. Z. Mutter, and J. Fang (1997), Shallow dips of normal faults during rapid extension: Earthquakes in the Woodlark-D'Entrecasteaux rift system, Papua New Guinea, *J. Geophys. Res.*, *102*, 15,301–15,317.

Altamimi, Z., P. Sillard, and C. Boucher (2002), ITRF2000: A new release of the International Terrestrial Reference Frame for earth science applications, *J. Geophys. Res.*, *107*(B10), 2214, doi:10.1029/2001JB000561.

Beavan, J., P. Tregoning, M. Bevis, T. Kato, and C. Meertens (2002), Motion and rigidity of the Pacific Plate and implications for plate boundary deformation, *J. Geophys. Res.*, *107*(B10), 2261, doi:10.1029/2001JB000282.

Benes, V., S. D. Scott, and R. A. Binns (1994), Tectonics of rift propagation into a continental margin: Western Woodlark Basin, Papua New Guinea, *J. Geophys. Res.*, *99*, 4439–4455.

Calmant, S., B. Pelletier, P. Lebellegard, M. Bevis, F. W. Taylor, and D. Phillips (2003), New insights on the tectonics along the New Hebrides subduction zone based on GPS results, *J. Geophys. Res.*, *108*(B6), 2319, doi:10.1029/2001JB000644.

Chapple, W. M., and T. E. Tullis (1977), Evaluation of the forces that drive the plates, *J. Geophys. Res.*, *82*, 1967–1984.

Chase, C. G. (1978), Extension behind island arcs and motions relative to hot spots, *J. Geophys. Res.*, *83*, 5385–5387.

Cooper, P., and B. Taylor (1987), Seismotectonics of New Guinea: A model for arc reversal following arc-continent collision, *Tectonics*, *6*, 53–67.

Curtis, J. W. (1973), Plate tectonics and the Papua New Guinea-Solomon Islands region, *J. Geol. Soc. Aust.*, *20*, 21–35.

Davies, H. L. (1971), Peridotite-gabbro-basalt complex in eastern Papua: An overthrust plate of oceanic mantle and crust, *Bur. Miner. Resour. Aust. Bull.*, *128*, 1–48.

Davies, H. L., P. A. Symonds, and I. D. Ripper (1984), Structure and evolution of the southern Solomon Sea region, *BMR J. Aust. Geol. Geophys.*, *9*, 49–68.

Davies, H. L., J. Lock, D. L. Tiffin, E. Honza, Y. Okuda, F. Murakami, and K. Kisimoto (1987), Convergent tectonics in the Huon Peninsula region, Papua New Guinea, *Geo Mar. Lett.*, *7*, 143–152.

DeMets, C., R. G. Gordon, D. F. Argus, and S. Stein (1990), Current plate motions, *Geophs. J. Int.*, *101*, 425–478.

DeMets, C., R. G. Gordon, D. F. Argus, and S. Stein (1994), Effects of recent revisions to the geomagnetic reversal time scale on estimates of current plate motions, *Geophys. Res. Lett.*, *21*, 2191–2194.

Denham, D. (1969), Distribution of earthquakes in the New Guinea-Solomon Islands region, *J. Geophys. Res.*, *74*, 4290–4299.

Dow, D. B. (1977), A geological synthesis of Papua New Guinea, *Bur. Miner. Resour. Aust. Bull.*, *201*, 1–41.

Dziewonski, A. M., and J. H. Woodhouse (1983), Studies of the seismic source using normal-mode theory, in *Earthquakes: Observation, Theory, and Interpretation: Notes from the International School of Physics 'Enrico Fermi'* (*1982: Varenna, Italy*), edited by H. Kanamori and E. Boscie, pp. 45–137, North-Holland, New York.

Elsasser, W. M. (1971), Sea-floor spreading as thermal convection, *J. Geophys. Res.*, *76*, 1101–1112.

England, P., and D. McKenzie (1982), A thin viscous sheet model for continental deformation, *Geophys. J. R. Astron. Soc.*, *70*, 295–321.

Falvey, D. A., and T. Pritchard (1982), Preliminary paleomagnetic results from northern Papua New Guinea: Evidence for large microplate rotations, in *Transactions of the Third Circum-Pacific Energy and Mineral Resources Conference*, pp. 593–599, Am. Assoc. of Pet. Geol., Tulsa, Okla.

Feigl, K., et al. (1993), Space geodetic measurements of crustal deformation in central and southern California, 1984–1992, *J. Geophys. Res.*, *98*, 21,677–21,712.

Forsyth, D., and S. Uyeda (1975), On the relative importance of the driving forces of plate motion, *Geophys. J. R. Astron. Soc.*, *43*, 163–200.

Goodliffe, A. M., B. Taylor, F. Martinez, R. Hey, K. Maeda, and K. Ohno (1997), Synchronous reorientation of the Woodlark basin spreading center, *Earth Planet. Sci. Lett.*, *146*, 233–242.

Hamilton, W. (1979), Tectonics of the Indonesian region, *U.S. Geol. Surv. Prof. Pap., 1078*, 345 pp.

Herring, T. A. (2001), GLOBK global Kalman filter VLBI and GPS analysis program, version 5.03, Mass. Inst. of Technol., Cambridge.

Herring, T. A., J. L. Davis, and I. I. Shapiro (1990), Geodesy by radio interferometry: The application of Kalman filtering to the analysis of very long baseline interferometry data, *J. Geophys. Res.*, *95*, 12,561–12,581.

Hill, K. C. (1991), Structure of the Papuan Fold Belt, Papua New Guinea, *AAPG Bull.*, *75*, 857–872.

Hill, K. C., and J. W. Gleadow (1989), Uplift and thermal history of the Papuan Fold Belt, Papua New Guinea: Apatite fission track analysis, *Aust. J. Earth Sci.*, *36*, 515–539.

Hill, K. C., and A. Raza (1999), Arc-continent collision in Papua New Guinea: Constraints from fission track thermochronology, *Tectonics*, *18*, 950–966.

Houseman, G., and P. England (1986), Finite strain calculations of continental deformation: 1. Method and general results for convergent zones, *J. Geophys. Res.*, *91*, 3651–3663.

Isacks, B., J. Oliver, and L. R. Sykes (1968), Seismology and the new global tectonics, *J. Geophys. Res.*, *73*, 5855–5899.

Jaques, A. L., and G. P. Robinson (1977), The continent/island-arc collision in northern Papua New Guinea, *BMR J. Aust. Geol. Geophys.*, *2*, 289–303.

Jenkins, D. A. (1974), Detachment tectonics in western Papua New Guinea, *Geol. Soc. Am. Bull.*, *85*, 533–548.
Johnson, R. W. (1979), Geotectonics and volcanism in Papua New Guinea: A review of the late Cainozoic, *BMR J. Aust. Geol. Geophys.*, *4*, 181–207.
Johnson, T., and P. Molnar (1972), Focal mechanisms and the tectonics of the southwest Pacific, *J. Geophys. Res.*, *77*, 5000–5032.
King, R. W., and Y. Bock (2002), Documentation for the GAMIT GPS analysis software, release 10.04, Mass. Inst. of Technol., Cambridge.
Kirchoff-Stein, K. S. (1992), Seismic reflection study of the New Britain and Trobriand subduction systems and their zone of initial contact in the western Solomon Sea, Ph.D. thesis, Univ. of Calif., Santa Cruz.
Kulig, C., R. McCaffrey, G. Abers, and H. Letz (1993), Shallow seismicity of arc-continent collision near Lae, Papua New Guinea, *Tectonophysics*, *227*, 81–93.
Mao, A., C. G. A. Harrison, and T. H. Dixon (1999), Noise in the GPS coordinate time series, *J. Geophys. Res.*, *104*, 2797–2816.
McCaffrey, R. (2002), Crustal block rotations and plate coupling, in *Plate Boundary Zones*, *Geodyn. Ser.*, vol. 30, edited by S. Stein and J. Freymueller, pp. 100–122, AGU, Washington, D. C.
McCaffrey, R., M. D. Long, C. Goldfinger, P. C. Zwick, J. L. Nabelek, C. K. Johnson, and C. Smith (2000), Rotation and plate locking at the southern Cascadia subduction zone, *Geophys. Res. Lett.*, *27*, 3117–3120.
McClusky, S., K. Mobbs, A. Stoltz, D. Barsby, W. Loratung, K. Lambeck, and P. Morgan (1994), The Papua New Guinea satellite crustal motion surveys, *Aust. Surv.*, *39*, 194–214.
McClusky, S., et al. (2000), Global Positioning System constraints on plate kinematics and dynamics in the eastern Mediterranean and Caucasus, *J. Geophys. Res.*, *105*, 5695–5719.
McKenzie, D., and J. Jackson (1983), The relationship between strain rates, crustal thickening, paleomagnetism, finite strain and fault movements within a deforming zone, *Earth Planet. Sci. Lett.*, *65*, 182–202.
McKenzie, D., and J. Jackson (1986), A block model of distributed deformation by faulting, *J. Geol. Soc. London*, *143*, 349–353.
Mobbs, K. (1997), Tectonic interpretation of the Papua New Guinea region from repeat satellite measurements, *Unisurv. Rep. S-48*, 256 pp., Univ. of New South Wales, Kennsington.
Molnar, P. (1988), Continental tectonics in the aftermath of plate tectonics, *Nature*, *335*, 131–137.
Molnar, P., and P. Tapponier (1975), Cenozoic tectonics of Asia: Effects of a continental collision, *Science*, *189*, 419–426.
Okada, Y. (1985), Surface deformation to shear and tensile faults in a half-space, *Bull. Seismol. Soc. Am.*, *75*, 1135–1154.
Pegler, G., S. S. Das, and J. H. Woodhouse (1995), A seismological study of the eastern New Guinea and the western Solomon Sea regions and its tectonic implications, *Geophys. J. Int.*, *122*, 961–981.
Pelletier, B., S. Calmant, and R. Pillet (1998), Current tectonics of the Tonga-New Hebrides region, *Earth Planet. Sci. Lett.*, *164*, 263–276.
Pigram, C. J., and H. L. Davies (1987), Terranes and the accretion history of the New Guinea orogen, *BMR J. Aust. Geol. Geophys.*, *10*, 193–211.
Press, W. H., B. P. Flannery, S. A. Teukolsky, and W. T. Vetterling (1989), *Numerical Recipes*, Cambridge Univ. Press, New York.
Reyners, M. (1998), Plate coupling and the hazard of large subduction thrust earthquakes at the Hikurangi subduction zone, New Zealand, *N. Z. J. Geol. Geophys.*, *41*, 343–354.
Ripper, I. D., and K. F. McCue (1983), The seismic zone of the Papuan fold belt, *J. Aust. Geol. Geophys.*, *8*, 147–156.
Ruellan, E., J. Delteil, I. Wright, and T. Matsumoto (2003), From rifting to active spreading in the Lau Basin-Havre Trough backarc system (SW Pacific): Locking/unlocking induced by seamount chain subduction, *Geochem. Geophys. Geosyst.*, *4*(5), 8909, doi:10.1029/2001GC000261.
Schouten, H., and V. Benes (1993), Post-Miocene collision along the Bismarck arc, western equatorial Pacific (abstract), *Eos Trans. AGU*, *74*(16), Spring Meet. Suppl., 286.
Schouten, H., K. D. Kiltgord, and D. G. Gallo (1993), Edge-driven microplate kinematics, *J. Geophys. Res.*, *98*, 6689–6701.
Silver, E. A., L. D. Abbott, K. S. Kirchoff-Stein, D. L. Reed, B. Bernstein-Taylor, and D. Hilyard (1991), Collision propagation in Papua New Guinea and the Solomon Sea, *Tectonics*, *10*, 863–874.
Soto-Cordero, L. (1998), Crustal processes associated with two slow convergent systems: The Trobriand trough, Papua New Guinea and the northern Panama deformed belt, M.S. thesis, 56 pp., Univ. of Calif., Santa Cruz.
Stevens, C., R. McCaffrey, E. A. Silver, Z. Sombo, P. English, and J. van der Kevie (1998), Mid-crustal detachment and ramp faulting in the Markham Valley, Papua New Guinea, *Geology*, *26*, 847–850.
Stevens, C., R. McCaffrey, Y. Bock, J. F. Genrich, Endang, C. Subarya, S. S. O. Puntodewo, Fauzi, and C. Vigny (1999), Rapid rotations about a vertical axis in a collisional setting revealed by the Palu Fault, Sulawesi, Indonesia, *Geophys. Res. Lett.*, *26*, 2677–2680.
Stevens, C., R. McCaffrey, Y. Bock, J. F. Genrich, M. Pubellier, and C. Subarya (2002), Evidence for block rotations and basal shear in the world's fastest slipping continental shear zone in NW New Guinea, in *Plate Boundary Zones*, *Geodyn. Ser.*, vol. 30, edited by S. Stein and J. Freymueller, pp. 87–99, AGU, Washington, D. C.
Taylor, B. (1979), Bismarck Sea: Evolution of a back-arc basin, *Geology*, *7*, 171–174.
Taylor, B., A. Goodliffe, and F. Martinez (1995), Continental rifting and initial seafloor spreading in the Woodlark Basin, *Nature*, *374*, 534–537.
Taylor, B., A. M. Goodliffe, and F. Martinez (1999), How continents break up: Insights from Papua New Guinea, *J. Geophys. Res.*, *104*, 7497–7512.
Tregoning, P. (2002), Plate kinematics in the western Pacific derived from geodetic observations, *J. Geophys. Res.*, *107*(B1), 2020, doi:10.1029/2001JB000406.
Tregoning, P., and H. McQueen (2001), Resolving slip vector azimuths and plate motion along the southern boundary of the South Bismarck Plate, Papua New Guinea, *Aust. J. Earth Sci.*, *5*, 745–760.
Tregoning, P., K. Lambeck, A. Stoltz, P. Morgan, S. C. McClusky, P. van der Beek, H. McQueen, R. J. Jackson, R. P. Little, A. Laing, and B. Murphy (1998), Estimation of current plate motions in Papua New Guinea from Global Positioning System observations, *J. Geophys. Res.*, *103*, 12,181–12,203.
Tregoning, P., R. J. Jackson, H. McQueen, K. Lambeck, C. Stevens, R. P. Little, R. Curley, and R. Rosa (1999), Motion of the South Bismarck Plate, Papua New Guinea, *Geophys. Res. Lett.*, *26*, 3517–3520.
Tregoning, P., H. McQueen, K. Lambeck, R. Jackson, R. Little, S. Saunders, and R. Rosa (2000), Present-day crustal motion in Papua New Guinea, *Earth Planets Space*, *52*, 727–730.
Viallon, C., P. Huchon, and E. Barrier (1986), Opening of the Okinawa basin and collision in Taiwan: A retreating trench model with lateral anchoring, *Earth Planet. Sci. Lett.*, *80*, 145–155.
Vilotte, J. P., M. Daignieres, and R. Madariaga (1982), Numerical modeling of intraplate deformation: Simple mechanical models of continental collision, *J. Geophys. Res.*, *87*, 10,709–10,728.
Weiler, P. D., and R. S. Coe (2000), Rotations in the actively colliding Finisterre-Arc Terrane: Paleomagnetic constraints on Plio-Pleistocene evolution of the South Bismarck microplate, northeastern Papua New Guinea, *Tectonophysics*, *316*, 297–325.
Weissel, J. K., B. Taylor, and G. D. Karner (1982), The opening of the Woodlark Basin, subduction of the Woodlark spreading system, and the evolution of northern Melanesia since mid-Pliocene time, *Tectonophysics*, *87*, 253–277.

R. Curley, S. Hasiata, and J. Taugaloidi, Papua New Guinea University of Technology, Private Mail Bag, Lae, Papua New Guinea. (r.curley@survey.unitech.ac.pg; s.hasiata@survey.unitech.ac.pg; j.taugaloidi@survey.unitech.ac.pg)

W. Loratung and R. Rosa, Papua New Guinea National Mapping Bureau, Private Mail Bag, Port Moresby, Papua New Guinea. (natmap@datec.com.pg)

R. McCaffrey, Department of Earth and Environmental Sciences, Rensselaer Polytechnic Institute, 110 8th St., Troy, NY 12180-3590, USA. (mccafr@rpi.edu)

R. Stanaway, Research School of Earth Sciences, Australian National University, Canberra ACT 0200, Australia. (rich@rses.anu.edu.au)

E. Silver, Earth Sciences Department, University of California, Santa Cruz, Applied Sciences Building, Santa Cruz, CA 95064-1077, USA. (esilver@es.ucsc.edu)

C. Stevens, Geographic Data Technology, 11 Lafayette Street, Lebanon, NH 03766, USA. (colleen_stevens@gdt1.com)

L. M. Wallace, Institute of Geological and Nuclear Sciences, Lower Hutt, New Zealand. (l.wallace@gns.cri.nz)